

## Parity Violation in $\vec{\gamma}p$ Compton Scattering

Jiunn-Wei Chen, Thomas D. Cohen

*Department of Physics, University of Maryland,  
College Park, MD 20742-4111*

`jwchen@physics.umd.edu, cohen@physics.umd.edu`

Chung Wen Kao

*Institut für Theoretische Physik, J. W. Goethe-Universität,  
60054 Frankfurt am Main, Germany*

`kaochung@th.physik.uni-frankfurt.de`

### Abstract

Polarized beam  $\vec{\gamma}p$  Compton scattering provides a theoretically clean way to extract the isovector parity violating pion-nucleon coupling constant  $h_{\pi NN}^{(1)}$ . This channel is more tractable experimentally than the recently proposed extraction of  $h_{\pi NN}^{(1)}$  from the Bedaque-Savage process — polarized target  $\gamma\vec{p}$  Compton scattering. The leading parity violating effect is calculated using Heavy Baryon Chiral Perturbation Theory ( $HB\chi PT$ ). The size of the asymmetry is estimated to be  $\sim 4 \times 10^{-8}$  for 120 MeV photon energy.

The isovector parity violating (PV) pion-nucleon coupling constant  $h_{\pi NN}^{(1)}$  is responsible for the longest range part of the  $\Delta I = 1$  PV  $NN$  forces [1–3]. It is expected to give dominant contributions to low energy quantities such as nucleon<sup>1</sup> and nuclear anapole moment [6–11], and PV neutron radiative capture  $np \rightarrow d\gamma$ . However, past attempts to extract  $h_{\pi NN}^{(1)}$  are not satisfactory (see [2,12,13] reviews). In many-body systems, several PV effects are enhanced and have been detected. On the other hand, the theoretical analysis is complicated. The extractions from  $^{18}F$  [14,15] and  $^{133}Cs$  [16–19] systems differ by an order of magnitude with large uncertainties, while the measurement in the  $^{205}Tl$  system gives a null result [20]. In fewer body systems, the theory is more under control but the PV effect is smaller such that previous measurements could not reach the required precision [21–24]. However there are several high precision new measurements under preparation or execution including  $\bar{\pi}^0 p \rightarrow d\gamma$  at LANSCE [25],  $\gamma d \rightarrow np$  at JLab [26], and the rotation of polarized neutrons in helium at NIST. It is expected that these experiments will put tight constraints on the value of  $h_{\pi NN}^{(1)}$ .

In the single nucleon system, a new PV observable was recently suggested by Bedaque and Savage [27]. They found that the polarized target  $\gamma \vec{p} \rightarrow \gamma p$  Compton scattering asymmetry measurement (calculated to be  $\sim 5 \times 10^{-8}$  for 100 MeV photon energy) would determine  $h_{\pi NN}^{(1)}$  with an estimated 15% uncertainty. To control systematic errors, the difference in cross section for the proton spin polarized parallel and antiparallel to the direction of the incident photon must be measured during a short period of time with only the target polarization direction changed. To achieve this, the rapid flipping of the target polarization should be employed. This is unpractical with the currently available experimental techniques and polarized proton targets, thus the Bedaque-Savage (BS) process is not favored experimentally. On the other hand, rapid flipping of beam helicity is a standard technique already employed in many parity violating experiments. Thus the polarized beam experiment,  $\vec{\gamma} p \rightarrow \gamma p$ , is experimentally more tractable [31]. Given the great interest in the determination of  $h_{\pi NN}^{(1)}$ , we investigate this  $\vec{\gamma} p$  parity violating process using Heavy Baryon Chiral Perturbation Theory ( $HB\chi PT$ ) [32,33].

We start with reviewing the symmetry constraints on the Compton scattering process

$$\gamma(k, \epsilon) + p \rightarrow \gamma(k', \epsilon') + p \quad , \quad (1)$$

where  $(k, \epsilon)$  and  $(k', \epsilon')$  are the initial and final photon momenta and polarization vectors. It has been known for a long time that there are ten time reversal invariant structure functions in the transition amplitude for this process. Six of them conserve parity while four of them violate parity. This can be seen easily by the following exercise on helicity amplitude counting. Using  $|\lambda_1, \lambda_2\rangle$  to denote a state with photon and proton helicity  $\lambda_1$  and  $\lambda_2$  in the center of mass frame, sixteen helicity amplitudes  $\langle \lambda'_1, \lambda'_2 | \lambda_1, \lambda_2 \rangle$  can be constructed for proton Compton scattering. These amplitudes transform under time reversal as

$$\langle \lambda'_1, \lambda'_2 | \lambda_1, \lambda_2 \rangle \xrightarrow{T} \langle \lambda_1, \lambda_2 | \lambda'_1, \lambda'_2 \rangle \quad , \quad (2)$$

---

<sup>1</sup> The isoscalar nucleon anapole moment is dominated by  $h_{\pi NN}^{(1)}$ , but not the isovector anapole moment which is more directly relevant for the SAMPLE electron-proton [4] and electron-deuteron [5] PV experiments.

which is equivalent to taking a transpose transformation of the  $4 \times 4$  matrix. Thus ten time reversal invariant amplitudes can be constructed through the linear combination

$$\mathcal{M}_T(\lambda_1, \lambda_2, \lambda'_1, \lambda'_2) = \langle \lambda'_1, \lambda'_2 | \lambda_1, \lambda_2 \rangle + \langle \lambda_1, \lambda_2 | \lambda'_1, \lambda'_2 \rangle \quad . \quad (3)$$

One can further separate these into PC and PV amplitudes. Two of the amplitudes,  $\mathcal{M}_T(+1, +1/2, -1, -1/2)$  and  $\mathcal{M}_T(+1, -1/2, -1, +1/2)$ , have an additional symmetry. They are invariant under parity transformation,

$$\langle \lambda'_1, \lambda'_2 | \lambda_1, \lambda_2 \rangle \xrightarrow{P} \langle -\lambda'_1, -\lambda'_2 | -\lambda_1, -\lambda_2 \rangle \quad , \quad (4)$$

after having been made to conserve time reversal invariance. The other eight amplitudes can be grouped into four PC and four PV amplitudes using similar linear combinations to that of eq.(3). This demonstrates the well-known result that there are six independent PC and four independent PV structure functions satisfying time-reversal invariance in a proton Compton scattering process.

In the center of mass frame, the six PC structure functions can be chosen as

$$\begin{aligned} T^{pc} = \bar{N} & \left[ \mathcal{A}_1 \epsilon \cdot \epsilon'^* + \mathcal{A}_2 \hat{\mathbf{k}} \cdot \epsilon'^* \hat{\mathbf{k}}' \cdot \epsilon + i\mathcal{A}_3 \sigma \cdot (\epsilon'^* \times \epsilon) + i\mathcal{A}_4 \sigma \cdot (\hat{\mathbf{k}}' \times \hat{\mathbf{k}}) \epsilon \cdot \epsilon'^* \right. \\ & + i\mathcal{A}_5 \sigma \cdot \left[ (\epsilon'^* \times \hat{\mathbf{k}}) \epsilon \cdot \hat{\mathbf{k}}' - (\epsilon \times \hat{\mathbf{k}}') \epsilon'^* \cdot \hat{\mathbf{k}} \right] \\ & \left. + i\mathcal{A}_6 \sigma \cdot \left[ (\epsilon'^* \times \hat{\mathbf{k}}') \epsilon \cdot \hat{\mathbf{k}} - (\epsilon \times \hat{\mathbf{k}}) \epsilon'^* \cdot \hat{\mathbf{k}}' \right] \right] N \quad , \quad (5) \end{aligned}$$

where  $N$  is the proton spinor,  $\sigma$  is the Pauli matrix acting on the nucleon spin index,  $\hat{\mathbf{k}}$  and  $\hat{\mathbf{k}}'$  are the unit vectors in the  $\mathbf{k}$  and  $\mathbf{k}'$  directions, and the Coulomb gauge ( $\epsilon_0 = \epsilon'_0 = 0$ ) is used. The PV structure functions can be chosen as

$$\begin{aligned} T^{pv} = \bar{N} & \left[ \mathcal{F}_1 \sigma \cdot (\hat{\mathbf{k}} + \hat{\mathbf{k}}') \epsilon \cdot \epsilon'^* - \mathcal{F}_2 \left( \sigma \cdot \epsilon'^* \hat{\mathbf{k}}' \cdot \epsilon + \sigma \cdot \epsilon \hat{\mathbf{k}} \cdot \epsilon'^* \right) \right. \\ & \left. - \mathcal{F}_3 \hat{\mathbf{k}} \cdot \epsilon'^* \hat{\mathbf{k}}' \cdot \epsilon \sigma \cdot (\hat{\mathbf{k}} + \hat{\mathbf{k}}') - i\mathcal{F}_4 \epsilon \times \epsilon'^* \cdot (\hat{\mathbf{k}} + \hat{\mathbf{k}}') \right] N \quad . \quad (6) \end{aligned}$$

The  $\mathcal{F}_{1-3}$  structures were first given in ref. [27]. The interference between  $\mathcal{A}_{1,2}$  and  $\mathcal{F}_{1-3}$  contributes to the BS process. For the polarized beam process  $\vec{\gamma}p \rightarrow \gamma p$  considered here, the contributions are from the interference between  $\mathcal{A}_{1,2}$  and  $\mathcal{F}_4$  and between  $\mathcal{A}_{3-6}$  and  $\mathcal{F}_{1-3}$ .

Since we are interested in the low energy behavior of the proton Compton scattering process, chiral perturbation theory provides a natural framework with which to work. As a low energy effective field theory of QCD, chiral perturbation theory captures the symmetries of QCD and describes low energy observables by derivative and Chiral expansions. The  $SU(2)_L \times U(1)$  symmetry structure of electroweak interactions can also be incorporated with the weak boson exchange described by contact interactions while keeping the photon as dynamical degrees of freedom in the Chiral Lagrangian.

$HB\chi PT$  has been applied to the calculation of several Compton scattering observables. The PC structure functions have been calculated up to next-to-leading order (NLO),  $\mathcal{O}(e^2 p)$  [33], and are listed in the Appendix. The proton Thompson term is the only contribution at leading order (LO) and contributes to  $\mathcal{A}_1$  only. The NLO contributions come from the tree level diagrams, pion-nucleon loop diagrams and the Wess-Zumino term. They contribute

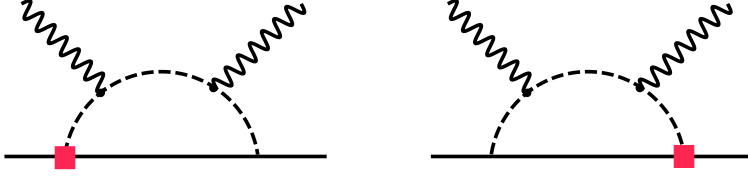


FIG. 1. The leading order contribution to parity violating structure functions  $\mathcal{F}_1$ - $\mathcal{F}_3$  in  $\gamma p$  Compton scattering. The solid square is the weak operator with coefficient  $h_{\pi NN}^{(1)}$ . Wavy lines are photons, solid lines are nucleons, and dashed lines are pions. The crossed graphs are not shown. Graphs with photons from the strong vertex, or insertion of the two-photon-pion vertex vanish in the  $v \cdot A = 0$  gauge, and thus are not shown here.

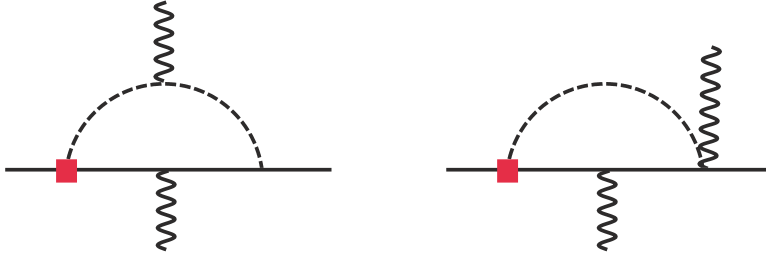


FIG. 2. The first non-vanishing order (NLO) contribution to parity violating structure functions  $\mathcal{F}_4$  in  $\gamma p$  Compton scattering. The features of the graphs are as defined in fig.1. The photon nucleon couplings are magnetic couplings.

to all the PC structure functions  $\mathcal{A}_{1-6}$ . These structure functions can be determined experimentally (see the Appendix for more details) thus the uncertainty from the PC part can be eliminated completely. Here we use the  $HB\chi PT$  result only for the sake of estimation of the asymmetry. For the PV structure functions, the LO ( $\mathcal{O}(G_F e^2)$  with  $G_F$  the Fermi coupling constant) contributions have been calculated in ref. [27]. We also list them in the Appendix. They arise from the pion loop diagrams shown in fig.1 and contribute to  $\mathcal{F}_1$ - $\mathcal{F}_3$ .  $\mathcal{F}_4$  is an additional quantity we will need to compute. Its contribution comes from the pion loop diagrams shown in fig.2 and the effect starts at NLO. Now we give some details of computing the  $\mathcal{F}_4^{NLO}$ .

The PC part of the relevant Lagrangian is

$$\begin{aligned} \mathcal{L}^{PC} = & \frac{1}{2} D_\mu \pi_i D^\mu \pi_i - \frac{m_\pi^2}{2} \pi_i^2 + i \bar{N} v_\mu D^\mu N - \frac{g_A}{F_\pi} \bar{N} S_\mu (D^\mu \pi_i) \tau_i N \\ & + \frac{1}{2M_N} \bar{N} [(v \cdot D)^2 - D^2] N - \frac{ie}{M_N} \bar{N} [S^\mu, S^\nu] [\mu_0 + \mu_1 \tau_3] N F_{\mu\nu} + \dots \end{aligned} \quad (7)$$

where the pion decay constant  $F_\pi = 93$  MeV, pion-nucleon coupling constant  $g_A = 1.26$ ,  $N$  is the isospin doublet of the nucleon fields with velocity  $v$ ,  $D$  is the covariant derivative with gauge coupling on the proton as  $D_\mu N = (\partial - ieA)_\mu N$ , and  $S$  is the covariant nucleon polarization vector. In the proton rest frame,  $v^\mu = (1, 0, 0, 0)$ ,  $S^\mu = (0, \sigma/2)$ .  $\mu_0 = (\mu_p +$

$\mu_n)/2$  and  $\mu_1 = (\mu_p - \mu_n)/2$  are the isoscalar and isovector magnetic moments in nuclear magnetons, with  $\mu_p = 2.79$  and  $\mu_n = -1.91$ . The ellipses denote terms with more pion fields and insertions of higher powers of derivative and pion mass. Massive hadronic excitations such as kaons and deltas are “integrated out”. Their effects are encoded in the higher dimensional operators.

The non-leptonic PV part of the relevant Lagrangian is

$$\mathcal{L}^{PV} = \frac{h_{\pi NN}^{(1)}}{\sqrt{2}} \varepsilon^{3ij} \bar{N} \pi_i \tau_j N + \dots = -i h_{\pi NN}^{(1)} \pi^+ p^\dagger n + h.c. + \dots \quad (8)$$

where the ellipses denote terms with more pion fields and derivatives. This Lagrangian was first given in ref. [3] with a different phase convention for the pion field. We adopt the same convention as refs. [10,11].  $h_{\pi NN}^{(1)}$  was estimated by matching onto four quark Fermi theory and was found to be dominated by  $s$  quark contributions,

$$\left| h_{\pi NN}^{(1)} \right| \sim \frac{G_F F_\pi \Lambda_\chi}{\sqrt{2}} \sim 5 \times 10^{-7} \quad , \quad (9)$$

where  $\Lambda_\chi \sim 1$  GeV is the chiral perturbation scale. This estimation is consistent with the “best value” obtained in ref. [1] and close to one result [28] from QCD sum rules. A recent calculation in the SU(3) Skyrme model yields  $h_{\pi NN}^{(1)} \sim 0.8\text{-}1.3 \times 10^{-7}$  [29]. The radiative correction on the  $h_{\pi NN}^{(1)}$  vertex is discussed in ref. [30].

The  $h_{\pi NN}^{(1)}$  term is the only term in the  $\mathcal{L}^{PV}$  with a non-derivative pion-nucleon coupling; it is expected to dominate over the other contributions to  $\mathcal{F}_4$ . The pion loop diagrams in fig.2 gives

$$\mathcal{F}_4^{NLO} = -\frac{e^2 g_A h_{\pi NN}^{(1)} \mu_n}{8\sqrt{2} m_N F_\pi \pi^2} \left[ \omega - \frac{m_\pi^2}{\omega} \left( \sin^{-1} \frac{\omega}{m_\pi} \right)^2 \right] \quad (10)$$

with a magnetic photon-nucleon coupling.  $\omega$  is the photon energy in the center-of-mass frame.

In this calculation delta contributions are encoded in the higher-order operators and will contribute through higher-order diagrams. If one considers the delta-nucleon mass difference  $\Delta \sim 300$  MeV as a light scale as  $m_\pi$  and  $\omega$  are, then one needs to sum factors of  $m_\pi/\Delta$  and  $\omega/\Delta$  to all orders. This can be done by including delta as a dynamical degree of freedom [32,34]. In this expansion, the delta diagrams will contribute to  $\mathcal{F}_{1-4}^{NLO}$  through  $\pi\Delta$  loop diagrams and tree diagrams with unknown  $\gamma N\Delta$  couplings. In the expansion with which we work, the  $\Delta$  is considered as a large or heavy scale, so factors of  $m_\pi/\Delta$  and  $\omega/\Delta$  are treated perturbatively. Thus below pion production threshold ( $\omega < m_\pi$ ), the delta would contribute a factor of  $(m_\pi^2/\Delta^2, \omega^2/\Delta^2) \sim 25\%$  correction to  $\mathcal{F}_4^{NLO}$ . This is the dominant source of the uncertainty.

The PV asymmetry can be defined by the difference in the cross section (in the center-of-mass frame) for photon helicity  $\lambda_\gamma = +1$  and  $-1$  normalized to the sum

$$A_{\gamma\gamma}(\omega, \theta) \equiv \frac{\frac{d\sigma}{d\Omega}(\lambda_\gamma = +1) - \frac{d\sigma}{d\Omega}(\lambda_\gamma = -1)}{\frac{d\sigma}{d\Omega}(\lambda_\gamma = +1) + \frac{d\sigma}{d\Omega}(\lambda_\gamma = -1)} \quad . \quad (11)$$

Again, the PC structure functions  $\mathcal{A}_{1-6}$  can be extracted from experiments to further reduce theoretical input and eliminate the uncertainties from the PC part. Here we plug in the PC  $HB\chi PT$  result in order to get an estimation of the size of the asymmetry. In this treatment, the helicity asymmetry contribution starts at NLO,

$$\begin{aligned}
A_{\gamma\gamma}(\omega, \theta) = & \frac{2 \sin^2 \theta}{|\mathcal{A}_1^{LO}|^2 (1 + \cos^2 \theta)} \text{Re} \{ \mathcal{A}_1^{LO} \mathcal{F}_4^{NLO*} + \mathcal{A}_3^{NLO} [\mathcal{F}_1^{LO*} - 2\mathcal{F}_2^{LO*} - \mathcal{F}_3^{LO*} (1 + \cos \theta)] \\
& + \mathcal{A}_5^{NLO} [\mathcal{F}_1^{LO*} (1 + \cos \theta) + \mathcal{F}_2^{LO*} (1 - 3 \cos \theta) + \mathcal{F}_3^{LO*} (1 - \cos^2 \theta)] \\
& - \mathcal{A}_6^{NLO} [\mathcal{F}_1^{LO*} (1 + \cos \theta) + \mathcal{F}_2^{LO*} (3 - \cos \theta) + \mathcal{F}_3^{LO*} (1 - \cos^2 \theta)] \\
& - \mathcal{A}_4^{NLO} \mathcal{F}_2^{LO*} (1 + \cos \theta) \} \\
& - \frac{4(1 + \cos \theta)}{|\mathcal{A}_1^{LO}|^2 (1 + \cos^2 \theta)} \text{Re} \{ \mathcal{A}_3^{NLO} \mathcal{F}_1^{LO*} + \mathcal{A}_1^{LO} \mathcal{F}_4^{NLO*} \} \quad . \quad (12)
\end{aligned}$$

We have used the LO result for the PC cross section, so

$$\frac{1}{2} \left[ \frac{d\sigma}{d\Omega}(\lambda_\gamma = +1) + \frac{d\sigma}{d\Omega}(\lambda_\gamma = -1) \right] = \frac{1}{2(4\pi)^2} |\mathcal{A}_1^{LO}|^2 (1 + \cos^2 \theta) = \frac{\alpha^2}{2M_N^2} (1 + \cos^2 \theta) \quad . \quad (13)$$

It is instructive to study the low energy limit ( $\omega \ll m_\pi$ ) of the asymmetry. Keeping the first term in the  $\omega/m_\pi$  expansion,

$$\begin{aligned}
\mathcal{A}_1^{LO} = & -\frac{e^2}{M_N} \quad , \quad \mathcal{A}_3^{NLO} \sim [1 + 2\kappa_p - (1 + \kappa_p)^2 \cos \theta] \frac{e^2 \omega}{2M_N^2} \quad , \\
\mathcal{A}_4^{NLO} = & -\mathcal{A}_5^{NLO} \sim -\frac{(1 + \kappa_p)^2 e^2 \omega}{2M_N^2} \quad , \quad \mathcal{A}_6^{NLO} \sim -\frac{(1 + \kappa_p) e^2 \omega}{2M_N^2} \quad , \\
\mathcal{F}_1^{LO*} = & \mathcal{F}_2^{LO*} \sim -\frac{e^2 g_A h_{\pi NN}^{(1)} \omega^2}{24\sqrt{2}\pi^2 F_\pi m_\pi^2} \quad , \quad \mathcal{F}_4^{NLO*} \sim +\frac{e^2 g_A h_{\pi NN}^{(1)} \mu_n \omega^3}{24\sqrt{2}\pi^2 F_\pi M_N m_\pi^2} \quad , \quad (14)
\end{aligned}$$

with  $\mathcal{F}_3^{LO*} = O(\omega^4/m_\pi^4)$  and  $\kappa_p \equiv \mu_p - 1$ . The inverse power of  $m_\pi$  dependence in the  $\mathcal{F}$ s explains why there are no intrinsic unknown two-photon-two-nucleon counterterms at this order. In this low energy limit, the asymmetry has a simple form

$$A_{\gamma\gamma}(\omega \ll m_\pi, \theta) = -\frac{g_A h_{\pi NN}^{(1)} [(2\mu_n + (\mu_p + 1)^2) \sin^2 \theta - 2(1 + \cos \theta) (2\mu_n - (\mu_p - 1)^2)] \omega^3}{24\sqrt{2}\pi^2 F_\pi m_\pi^2 (1 + \cos^2 \theta)} \quad (15)$$

$$\cdot \left( 1 + \mathcal{O} \left( \frac{\omega^2}{m_\pi^2}, \frac{m_\pi^2}{\Delta^2} \right) \right) \quad . \quad (16)$$

The vanishing of  $A_{\gamma\gamma}$  at backward angle ( $\theta = \pi$ ) is a consequence of time-reversal invariance and is a general property for all values of the photon energy. For back scattering, the change of photon spin direction corresponds to a  $\Delta J = 2$  operation and hence, is a forbidden transition for the proton matrix element. Thus both photon and proton spin directions do not change but the helicities change signs. Using eq.(3) for the time-reversal invariant amplitude and  $(\lambda'_1, \lambda'_2) = (-\lambda_1, -\lambda_2)$ , this amplitude conserves parity and does not contribute to the PV asymmetry.

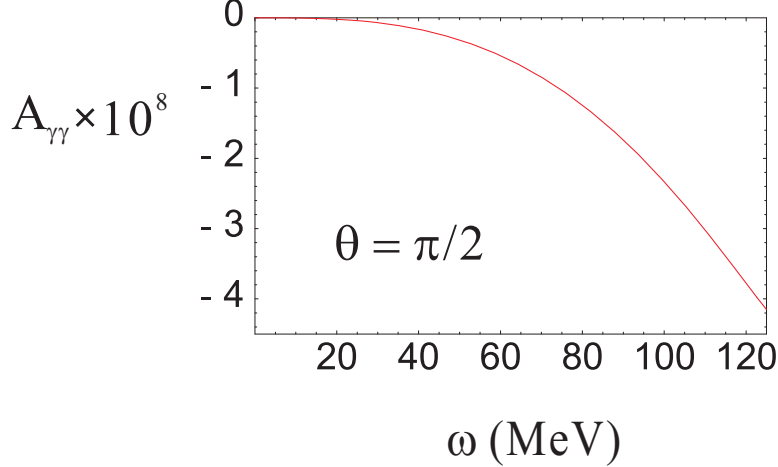


FIG. 3. The estimated photon helicity asymmetry  $A_{\gamma\gamma}$  defined in eq.(11) shown as a function of photon energy with the photon reflection angle  $\theta = \pi/2$  in the center-of-mass-frame. The naively estimated value of  $h_{\pi NN}^{(1)} = 5 \times 10^{-7}$  is taken as input, and a  $HB\chi PT$  estimation used for the parity conserving amplitude.

For a numerical estimation of the magnitude of the asymmetry, we consider  $\theta = \pi/2$ , where

$$A_{\gamma\gamma} \left( \omega \ll m_\pi, \frac{\pi}{2} \right) \sim -8.8 \times 10^{-9} \left( \frac{h_{\pi NN}^{(1)}}{5 \times 10^{-7}} \right) \left( \frac{\omega}{70 \text{ MeV}} \right)^3 \quad (17)$$

with  $\sim 25\%$  uncertainty.

In fig.3, we show the photon energy dependence of the estimated asymmetry at  $\theta = \pi/2$ . Assuming the naive size for  $h_{\pi NN}^{(1)}$  estimated in eq.(9), the asymmetry is  $A_{\gamma\gamma}(120 \text{ MeV}, \pi/2) \sim -3.8 \times 10^{-8}$ , with the higher-order uncertainty  $\sim (m_\pi^2/\Delta^2, \omega^2/\Delta^2) \sim 25\%$ . Note that very near the pion production threshold, resummation of terms with powers of

$$\frac{m_\pi^2}{2m_N(\omega - m_\pi)} \quad (18)$$

is required in order to shift the pion production threshold from  $m_\pi$  to  $m_\pi + \frac{m_\pi^2}{2m_N}$  (in the laboratory frame) to recover the recoil effect. The resummation procedure is well known [35]. Without this resummation, we should restrict ourselves to  $\omega < 130 \text{ MeV}$  such that the factor in (18) is sufficiently less than 1. To probe how far away from the threshold our calculation is still under control, we compare the results of expanding the  $A_{\gamma\gamma}$  to NLO to that of expanding the total amplitude to NLO, then square it to get the  $A_{\gamma\gamma}$  (the  $\mathcal{A}_2 \mathcal{F}_4$  interference term is included in the latter case). If the difference between these two quantities is consistent with the estimated higher order contribution, then the result without extra resummation will be valid. We find the difference increases with  $\omega$  and reaches 14% at  $\omega = 120 \text{ MeV}$ , so our expansion is presumably still useful up to 120 MeV.

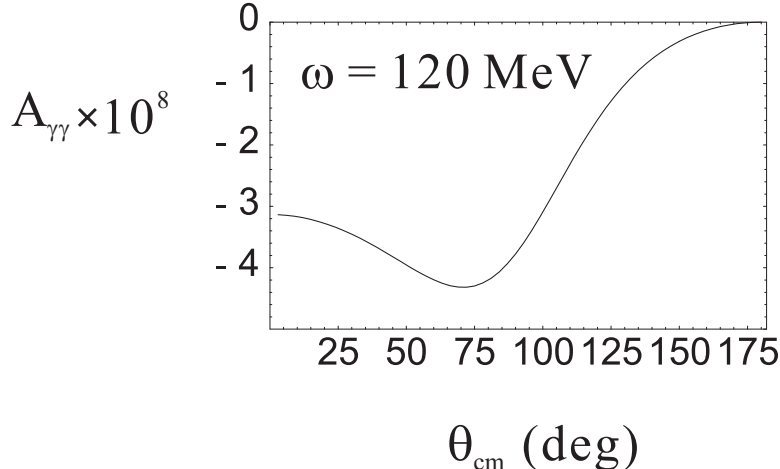


FIG. 4. The angular distribution of the estimated photon helicity asymmetry  $A_{\gamma\gamma}$  defined in eq.(11) and calculated in  $HB\chi PT$  in the center-of-mass-frame for 100 MeV photon energy. The naively estimated value of  $h_{\pi NN}^{(1)} = 5 \times 10^{-7}$  is taken as input.

In fig.4, we show the angular distribution at  $\omega = 120$  MeV for the same estimated value of  $h_{\pi NN}^{(1)}$ . The maximum asymmetry is near  $\theta = \pi/2$  but slightly biased towards the forward direction. The asymmetry vanishes at  $\theta = \pi$  as required by time reversal invariance.

In conclusion, parity violating  $\vec{\gamma}p \rightarrow \gamma p$  Compton scattering provides a theoretically clean way to extract  $h_{\pi NN}^{(1)}$ . The dominating source of the PV effect comes from the PV pion loop contributions. The magnitude of the helicity asymmetry is estimated to be  $\sim 4 \times 10^{-8}$  at 120 MeV photon energy with  $\sim 25\%$  uncertainty for a natural size  $h_{\pi NN}^{(1)}$ , under the framework of  $HB\chi PT$ . Thus we have found a model independent way to constrain  $h_{\pi NN}^{(1)}$  with  $\sim 25\%$  uncertainty. We note that the  $\sim 25\%$  uncertainty is dominantly due to the delta and can in principle be reduced by inclusion of the delta as an explicit degree of freedom. Unfortunately this would require additional experiments to measure the PV  $\gamma N \Delta$  coupling. However, even with  $\sim 25\%$  uncertainties,  $\vec{\gamma}p$  Compton scattering will greatly improve our understanding of  $h_{\pi NN}^{(1)}$ . We are optimistic that this experiment is feasible for current experimental techniques and facilities.

## ACKNOWLEDGMENTS

J.W.C. and T.D.C. thank the Institute for Nuclear Theory at the University of Washington for its hospitality and the Department of Energy for partial support during the completion of this work. J.W.C. thanks P. Bedaque, T. Hemmert, X. Ji, U. Meissner, M. Ramsey-Musolf, M. Savage, R. Springer, and R. Suleiman for useful discussions. J.W.C. and T.D.C. are supported in part by the U.S. Dept. of Energy under grant No. DE-FG02-93ER-40762. C.W.K is supported by the Alexander von Humboldt Foundation.



## Appendix

The following PC structure functions computed to  $\mathcal{O}(e^2p)$  are taken from eqs. (4.28a-g) of ref. [33] (with a typo in eq.(4.28b) corrected).

$$\begin{aligned} \mathcal{A}_1^{LO} &= -\frac{e^2}{M_N} \\ \mathcal{A}_1^{NLO} &= \frac{g_A^2 e^2}{8\pi F_\pi^2} \left\{ m_\pi - \sqrt{m_\pi^2 - \omega^2} + \frac{2M_\pi^2 - t}{\sqrt{-t}} \left[ \frac{1}{2} \arctan \frac{\sqrt{-t}}{2m_\pi} \right. \right. \\ &\quad \left. \left. - \int_0^1 dz \arctan \frac{(1-z)\sqrt{-t}}{2\sqrt{M_\pi^2 - \omega^2 z^2}} \right] \right\} \end{aligned} \quad (19)$$

$$\mathcal{A}_2^{NLO} = \frac{e^2 \omega}{M_N^2} + \frac{e^2 g_A^2 \omega^2 t - 2m_\pi^2}{8\pi F_\pi^2 (-t)^{3/2}} \int_0^1 dz \left[ \arctan \frac{(1-z)\sqrt{-t}}{2\sqrt{m_\pi^2 - \omega^2 z^2}} - \frac{2(1-z)\sqrt{t(\omega^2 z^2 - m_\pi^2)}}{4m_\pi^2 - 4\omega^2 z^2 - t(1-z)^2} \right] \quad (20)$$

$$\begin{aligned} \mathcal{A}_3^{NLO} &= \frac{e^2 \omega}{2M_N^2} [1 + 2\kappa_p - (1 + \kappa_p)^2 \cos \theta] + \frac{e^2 g_A t \omega}{8\pi^2 F_\pi^2 (m_\pi^2 - t)} + \frac{e^2 g_A^2}{8\pi^2 F_\pi^2} \left[ \frac{M_\pi^2}{\omega} \arcsin^2 \frac{\omega}{m_\pi} - \omega \right] \\ &\quad + \frac{e^2 g_A^2}{4\pi^2 F_\pi^2} \omega^4 \sin^2 \theta \int_0^1 dx \int_0^1 dz \frac{x(1-x)z(1-z)^3}{W^3} \left[ \arcsin \frac{\omega z}{R} + \frac{\omega z W}{R^2} \right] \end{aligned} \quad (21)$$

$$\mathcal{A}_4^{NLO} = -\frac{e^2(1 + \kappa_p)^2 \omega}{2M_N^2} + \frac{e^2 g_A^2}{4\pi^2 F_\pi^2} \int_0^1 dx \int_0^1 dz \frac{z(1-z)}{W} \arcsin \frac{\omega z}{R} \quad (22)$$

$$\begin{aligned} \mathcal{A}_5^{NLO} &= \frac{e^2 \omega}{2M_N^2} (1 + \kappa_p)^2 - \frac{e^2 g_A \omega^3}{8\pi^2 F_\pi^2 (m_\pi^2 - t)} + \frac{e^2 g_A^2 \omega^2}{8\pi^2 F_\pi^2} \int_0^1 dx \int_0^1 dz \left[ -\frac{(1-z)^2}{W} \arcsin \frac{\omega z}{R} \right. \\ &\quad \left. + 2\omega^2 \cos \theta \frac{x(1-x)z(1-z)^3}{W^3} \left( \arcsin \frac{\omega z}{R} + \frac{\omega z W}{R^2} \right) \right] \end{aligned} \quad (23)$$

$$\begin{aligned} \mathcal{A}_6^{NLO} &= -\frac{e^2 \omega}{2M_N^2} (1 + \kappa_p) + \frac{e^2 g_A \omega^3}{8\pi^2 F_\pi^2 (m_\pi^2 - t)} + \frac{e^2 g_A^2 \omega^2}{8\pi^2 F_\pi^2} \int_0^1 dx \int_0^1 dz \left[ \frac{(1-z)^2}{W} \arcsin \frac{\omega z}{R} \right. \\ &\quad \left. - 2\omega^2 \frac{x(1-x)z(1-z)^3}{W^3} \left( \arcsin \frac{\omega z}{R} + \frac{\omega z W}{R^2} \right) \right] \end{aligned} \quad (24)$$

with

$$\begin{aligned} t &= (k - k')^2 = -2\omega^2 (1 - \cos \theta), \\ W &= \sqrt{m_\pi^2 - \omega^2 z^2 + t(1-z)^2 x(x-1)}, \quad R = \sqrt{m_\pi^2 + t(1-z)^2 x(x-1)}. \end{aligned} \quad (25)$$

Expressions of PC Compton scattering for the unpolarized differential cross section,  $d\sigma/d\Omega$ , proton-photon spin parallel asymmetry  $\mathcal{A}_\parallel$ , and proton-photon spin perpendicular asymmetry  $\mathcal{A}_\perp$  are given in terms of PC structure functions in eqs.(4.18) and (4.19) of ref. [33]. These structure functions can be extracted experimentally. For example, below pion

production threshold ( $\omega < m_\pi$ ), one can extract  $\mathcal{A}_1$  and  $\mathcal{A}_3$  by measuring  $d\sigma/d\Omega$  and  $\mathcal{A}_\parallel$  at  $\theta = 0$ . Since  $\mathcal{A}_i$  are all real below pion production threshold and  $\mathcal{A}_\parallel \propto \mathcal{A}_1^2 + \mathcal{A}_3^2$  and  $\mathcal{A}_\perp \propto \mathcal{A}_1\mathcal{A}_3$ , measurements of  $\mathcal{A}_\parallel$  and  $\mathcal{A}_\perp$  are sufficient to extract  $\mathcal{A}_1$  and  $\mathcal{A}_3$ .

The following PV structure functions are given by ref. [27].

$$\begin{aligned}
\mathcal{F}_1(\omega, \theta) &= \frac{e^2 g_A h_{\pi NN}^{(1)}}{4\sqrt{2}\pi^2 F_\pi} \int_0^1 dx \int_0^{1-x} dy (1-2y)\omega [\mathcal{I}(-1; x\omega, \tilde{m}^2) - \mathcal{I}(-1; -x\omega, \tilde{m}^2)] \\
\mathcal{F}_2(\omega, \theta) &= \frac{e^2 g_A h_{\pi NN}^{(1)}}{2\sqrt{2}\pi^2 F_\pi} \int_0^1 dx \int_0^{1-x} dy y \omega [\mathcal{I}(-1; x\omega, \tilde{m}^2) - \mathcal{I}(-1; -x\omega, \tilde{m}^2)] \\
\mathcal{F}_3(\omega, \theta) &= \frac{e^2 g_A h_{\pi NN}^{(1)}}{2\sqrt{2}\pi^2 F_\pi} \int_0^1 dx \int_0^{1-x} dy y (1-x-y) (2y-1)\omega^3 [\mathcal{I}(-2; x\omega, \tilde{m}^2) - \mathcal{I}(-2; -x\omega, \tilde{m}^2)] \\
\tilde{m}^2 &= m_\pi^2 + 2y(1-x-y) \omega^2 (1 - \cos\theta) \quad , \tag{26}
\end{aligned}$$

where the functions  $\mathcal{I}(\alpha; b, c)$  are defined by Jenkins and Manohar in ref. [32]

$$\begin{aligned}
\mathcal{I}(\alpha; b, c) &= \int_0^\infty d\lambda (\lambda^2 + 2\lambda b + c)^\alpha \\
\mathcal{I}(-1; \Delta, m^2) &= -\frac{1}{2\sqrt{\Delta^2 - m^2 + i\epsilon}} \log \left( \frac{\Delta - \sqrt{\Delta^2 - m^2 + i\epsilon}}{\Delta + \sqrt{\Delta^2 - m^2 + i\epsilon}} \right) \\
\mathcal{I}(-2; \Delta, m^2) &= \frac{1}{2(\Delta^2 - m^2 + i\epsilon)} \left( \frac{\Delta}{m^2} - \mathcal{I}(-1; \Delta, m^2) \right) \quad . \tag{27}
\end{aligned}$$

## REFERENCES

- [1] B. Desplanques, J.F. Donoghue and B.R. Holstein, *Ann. Phys. (N.Y.)* **124**,449 (1980).
- [2] E.G. Adelberger and W.C. Haxton, *Ann. Rev. Nucl. Part. Sci.* **35**, 501 (1985).
- [3] D.B. Kaplan and M.J. Savage, *Nucl. Phys. A* **556**, 653 (1993).
- [4] D.T. Spayde et al., the SAMPLE Collaboration, *Phys. Rev. Lett.* **84**, 1106 (2000).
- [5] Bates experiment #94-11 (M. Pitt and E.J. Beise, contacts); M. Pitt and E.J. Beise, private communication.
- [6] Y.B. Zel'dovich, *Sov. Phys. JETP* **6**, 1184 (1958); *Sov. Phys. JETP* **12**, 777 (1961).
- [7] W.C. Haxton, E.M. Henley and M.J. Musolf, *Phys. Rev. Lett.* **63**, 949 (1989).
- [8] M.J. Musolf and B.R. Holstein, *Phys. Rev. D* **43**, 2956 (1991).
- [9] M.J. Savage and R.P. Springer *Nucl. Phys. A* **644**, 635 (1998), *Erratum-ibid. A* **657**, 457 (1999); `nucl-th/9907069`.
- [10] C.M. Maekawa and U. van Kolck, *Phys. Lett. B* **478**, 73 (2000); C.M. Maekawa, J.S. Veiga and U. van Kolck, *Phys. Lett. B* **488**, 167 (2000).
- [11] S.-L. Zhu, S.J. Puglia, B.R. Holstein and M.J. Ramsey-Musolf, *Phys. Rev. D* **62**, 033008 (2000).
- [12] W. Haeberli, B.R. Holstein, in *Symmetries and Fundamental Interactions in Nuclei*, ed. W.C. Haxton and E.M. Henley (World Scientific, Singapore, 1995), p.17.
- [13] W.T.H. van Oers, *Int. J. Mod. Phys. E* **8**, 417 (1999), `hep-ph/9910328`.
- [14] S.A. Page *et al.*, *Phys. Rev. C* **35**, 1119 (1987).
- [15] M. Bini, T. F. Fazzini, G. Poggi, and N. Taccetti, *Phys. Rev. C* **38**, 1195 (1988).
- [16] C.S. Wood et al., *Science* **275**, 1759 (1997).
- [17] W.C. Haxton, *Science* **275**,1753 (1997).
- [18] V.V. Flambaum and D.W. Murray, *Phys. Rev. C* **56**, 1641 (1997).
- [19] W.S. Wilburn and J.D. Bowman, *Phys. Rev. C* **57**, 3425 (1998).
- [20] P.A. Vetter *et al.*, *Phys. Rev. Lett.* **74**, 2658 (1995).
- [21] V.A. Knyazkov *et al.*, *Nucl. Phys. A* **417**, 209 (1984).
- [22] J.F. Cavagnac, B. Vignon and R. Wilson, *Phys. Lett. B* **67**, 148 (1997); J. Alberi *et al.*, in *Proceedings of the Symposium/Workshop on Spin and Symmetries*, ed. W.D. Ramsay and W.T.H. van Oers, *Can. J. Phys.* **66**, 542 (1988).
- [23] E.D. Earle et al., in *Proceedings of the Symposium/Workshop on Spin and Symmetries*, ed. W.D. Ramsay and W.T.H. van Oers, *Can. J. Phys.* **66**, 534 (1988).
- [24] D.M. Markoff, Ph.D. Thesis, University of Washington (1997).
- [25] W.M. Snow et al., *Nucl. Inst. Meth. A* **440**, 729 (2000).
- [26] JLab LOI 00-002, W. van Oers and B. Wojtsekhowski, spokesmen.
- [27] P.F. Bedaque and M.J. Savage, *Phys. Rev. C* **62** 018501 (2000).
- [28] E.M. Henley, W.-Y.P. Hwang and L.S. Kisslinger, *Phys. Lett. B* **367**, 21(1999); *Erratum-ibid. B* 440, 449 (1998).
- [29] U.G. Meissner and H. Weigel, *Phys. Lett. B* **447**, 1 (1999).
- [30] S.-L. Zhu, S.J. Puglia, B.R. Holstein and M.J. Ramsey-Musolf, `hep-ph/0008140`.
- [31] R. Suleiman, private communication.
- [32] E. Jenkins and A. V. Manohar, *Phys. Lett. B* **255**, 558 (1991); Lectures given at the *Workshop on Effective Field Theories of the Standard Model*, Dobogoko, Hungary, Aug 1991. In \*Dobogokoe 1991, Proceedings, *Effective field theories of the standard model* pages 113-137.

- [33] V. Bernard, N. Kaiser and Ulf-G. Meissner, *Int. J. Mod. Phys. E* **4** (1995) 193.
- [34] T.R. Hemmert, B.R. Holstein and J. Kambor, *Phys. Lett. B* **395**, 89 (1997).
- [35] T. Becher and H. Leutwyler, *Eur. Phys. J. C* **9**, 643 (1999).